Combination of miR-143 and miR-506 reduces lung and pancreatic cancer cell growth through the downregulation of cyclin-dependent kinases

A.K.M. NAWSHAD HOSSIAN[1], GERARDO G. MACKENZIE[2] and GEORGE MATTHEOLABAKIS[1]

[1]School of Basic Pharmaceutical and Toxicological Sciences, College of Pharmacy, University of Louisiana Monroe, Monroe, LA 71201; [2]Department of Nutrition, University of California Davis, Davis, CA 95616, USA

Received June 22, 2020; Accepted December 24, 2020

DOI: 10.3892/or.2021.7953

Abstract. Lung cancer (LC) and pancreatic cancer (PC) are the first and fourth leading causes of cancer-related deaths in the US. Deregulated cell cycle progression is the cornerstone for rapid cell proliferation, tumor development, and progression. Here, we provide evidence that a novel combinatorial miR treatment inhibits cell cycle progression at two phase transitions, through their activity on the *CDK4* and *CDK1* genes. Following transfection with miR-143 and miR-506, we analyzed the differential gene expression of *CDK4* and *CDK1*, using qPCR or western blot analysis, and evaluated cell cycle inhibition, apoptosis and cytotoxicity. The combinatorial miR-143/506 treatment downregulated CDK4 and CDK1 levels, and induced apoptosis in LC cells, while sparing normal lung fibroblasts. Moreover, the combinatorial miR treatment demonstrated a comparable activity to clinically tested cell cycle inhibitors in inhibiting cell cycle progression, by presenting substantial inhibition at the G_1/S and G_2/M cell cycle transitions. More importantly, the miR-143/506 treatment presented a broader application, effectively downregulating CDK1 and CDK4 levels, and reducing cell growth in PC cells. These findings suggest that the miR-143/506 combination acts as a promising approach to inhibit cell cycle progression for cancer treatment with minimal toxicity to normal cells.

Introduction

Despite the recent developments in novel therapeutics and improvements in early detection, the 5-year survival rates for lung cancer (LC) and pancreatic cancer (PC) patients remain at 19 and 9%, respectively. To date, these two diseases are the first and fourth most common cancer-related deaths in the US (1). These data establish the magnitude of the clinical problem, underlying the need for identifying novel therapeutic approaches.

Dysregulated cell cycle progression and rapid cell proliferation is a common attribute of cancer cells (2,3). In normal cells, the sequential progression through the stages of the cell cycle is regulated by the differential expression and activation of proteins, with cyclins and cyclin-dependent kinases (CDKs) playing a central role (4). The activity of the cyclin/CDK complexes prevents the premature entry of cells into the cell cycle and ensure its appropriate progression. In cancer cells, these highly conserved pathways are believed to enable the viability of cancer cells in the face of deregulated cellular proliferation (5) and consequently have been identified as therapeutic targets for cancer treatment (4). For example, numerous clinical trials have taken place using molecules that inhibit the activity of CDKs and block cell cycle progression. Recently, three such molecules (ribociclib, palbociclib and abemaciclib) were approved for the treatment of hormone receptor-positive, epidermal growth factor receptor 2 (EGFR2)-negative metastatic breast cancer (6-12).

G_1/S transition of the cell cycle is associated with the activity of CDK4/6. In LC, CDK4 has an elevated expression, which negatively correlates to prognosis (13), while CDK6 has been reported to be either upregulated or downregulated in different subtypes of LC (14). Early research on halting G_1/S cell cycle transition using CDK4 inhibition has been promising, with induced apoptotic activity and tumor growth inhibition (15,16). Unfortunately, clinical trials have indicated that CDK4/6 monotherapy is unlikely to exert sufficient therapeutic outcomes, even in cases with CDK4/6 activation (17).

Similar to LC, PC displays a broad spectrum of genetic alterations that drive the cancer phenotype and supports uncontrolled proliferation. For example, activating *KRAS*, observed in >90% of cases (18,19), drives deregulated proliferation and activates survival signals, but can also elicit replication stress, induction of reactive oxygen species, and promote oncogene-induced senescence (20,21). Rapid proliferation and deregulated cell cycle progression are also observed in PC, which is associated with the activation of the CDKs (22). CDKs

Correspondence to: Dr George Mattheolabakis, School of Basic Pharmaceutical and Toxicological Sciences, College of Pharmacy, University of Louisiana Monroe, 1800 Bienville Drive, Monroe, LA 71201, USA
E-mail: matthaiolampakis@ulm.edu

Key words: miR-143, miR-506, lung cancer, pancreatic cancer, cell cycle

are upregulated in PC, and their expression is also negatively correlated with chemoresistance and prognosis (23). Efforts to regulate the cell cycle in PC through CDK inhibitors, focusing primarily on halting the G_1/S transition have taken place (22). Still, PC exhibits intrinsic resistance to CDK4/6 inhibition mediated through a KRAS-dependent response and blocking of the Rb tumor suppressor activity (23,24), which can also lead to increased metastatic potential (25).

Thus, although inducing a G_1/S transition halt can be a promising approach for cancer treatment, combination therapies targeting complementary modulators of the cell cycle are required to overcome these limitations in LC and PC (26). During cell cycle progression, transitioning from G_2 to M phase is a crucial step for the successful mitosis process. CDK1 is a critical protein for that transition and the completion of cell cycle progression (8,27,28). Furthermore, CDK1 expression is increased in LC and PC samples, with a negative correlation to survival rates (29-31), also classifying this protein as a predictive biomarker and potential target for treatment in these two cancers (29,32). Targeting two cell cycle transitions, at the G_1/S and G_2/M represents a highly significant strategy for LC and PC therapy.

miR-based therapeutics have emerged as promising mRNA regulators for cancer treatment, capable to control multiple cell functions (33). In particular, the miR combination of miR-143 and miR-506 inhibits the cell cycle progression in two phase transitions, through downregulation of CDK1, CDK4 and CDK6, and causes strong apoptotic activity, as we recently reported (34,35). Here, we report on the combinatorial treatment effect of these two miRs downregulating CDK1, CDK4 and CDK6, and inhibiting cell growth in LC and PC cells. Our analysis reveals the efficacy and activity of the combinatorial miR-143/506 treatment with broader implications in LC and PC.

Materials and methods

Materials. Cell culture reagents were obtained from Gibco™ (Thermo Fisher Scientific, Inc.) and VWR International, LLC. miR-143-3p and miR-506-3p mimics were purchased from ABM. Negative control scramble-siRNA was purchased from Ambion. Opti-MEM and Lipofectamine 2000 reagent were obtained from Thermo Fisher Scientific, Inc., and the Quick-RNA miniprep kit was obtained from Zymo Research. Rabbit polyclonal anti-human CDK1 (dilution: 1:10,000; product #ab140847), rabbit monoclonal anti-human CDK4 (dilution: 1:2,000; product #ab108357), rabbit polyclonal anti-human β-tubulin (dilution: 1:500; product #ab6046), and goat anti-rabbit IgG H&L (HRP) secondary (dilution: 1:10,000; product #ab97051) antibodies were purchased from Abcam. Other chemicals and kits were purchased from Thermo Fisher Scientific, Inc., VWR, or Sigma-Aldrich/Merck KGaA. H69-AR, Calu3, H358, and H1975 LC cell lines, normal fibroblast cell line HFL-1, MIA-Paca-2, and Panc-1 PC cell lines were obtained from and cultured according to ATCC. Cells were accordingly cultured with DMEM, F12K media, or RPMI-1640 media supplemented with 10% fetal bovine serum (FBS) and 1% penicillin/streptomycin, at 37˚C with 5% CO_2.

Cell culture and transfection. We transfected the respective cells with miR-143(-3p), and miR-506(-3p) mimics or scrambled siRNA, using Lipofectamine 2000, following the manufacturer's protocol and as previously described (34,35). Briefly, H358 and H1975 LC cells were cultured in RPMI medium. MIA-Paca-2 and Panc-1 PC cells were cultured in DMEM supplemented with 10% fetal serum and 1% penicillin/streptomycin. Although these cells lines were not authenticated in our laboratory they were characterized by cell morphology and growth rate, and cultured in our laboratory less than six months after being received. For different experiments, the cells were seeded overnight in T25 cm^2 flask/6well/96-well plates, accordingly, and we transfected them with the respective miR mimics or scramble at 100 nM using Lipofectamine 2000, for 6 h, and the media were subsequently replaced with fresh media for incubation of up to 48 h.

Quantitative real-time qPCR (qPCR) analysis. We isolated total RNA using the Quick-RNA Miniprep kit and used Verso cDNA Synthesis Kit to develop complementary DNA to performed quantitative RT-qPCR using PowerUP SYBR-Green Master Mix (Applied Biosystems/Thermo Fisher Scientific, Inc.), as previously described (34,35). In Table SI, we present the primer sequences used for the detection of *CDK1*, *CDK4*, *CDK6*, and *CYPA*. We normalized all of the results to the untreated cells and calculated differential gene expression using the -ΔΔCq method (36). Scrambled siRNA with Lipofectamine were used as a negative control. All P-values are in comparison to untreated (control) samples unless stated otherwise.

Western blot analysis. We performed western blot (WB) analysis on protein extracts from H358, H1975, MIA-Paca-2, and Panc-1 cells, following previously established protocols (34,35). Briefly, protein extracts from the cells transfected with miR-143 and/or miR-506 for 24 and/or 48 h were aliquoted. We used 10-12% (w/v) polyacrylamide gel electrophoresis to separate proteins according to their size and transferred them to PVFD membranes, followed by incubation with the respective antibodies to detect CDK1, CDK4 or β-tubulin. After incubation at room temperature with the secondary antibody, we identified the protein bands using chemiluminescent substrate, visualized under a Chemidoc imaging system (Bio-Rad Laboratories, Inc.). We performed the histogram analysis using BioRad Image Lab V-6.0 software (Bio-Rad Laboratories, Inc.).

Cell cycle assay. We performed the cell cycle analysis using a flow cytometric technique, as previously described (34,35). Briefly, we stained cells with propidium iodide (PI) (MP Biomedicals, LLC) and analyzed the cells using a BD FACSCalibur Flow Cytometer, with Cellquest Pro software (BD Biosciences). We measured 10,000 events of the gated population. We identified the percentage of cell distributions in the various cell cycle phases using ModFit LT 5.0 (Verity Software House).

Apoptosis assay. We harvested H358, H1975, and HFL-1 cells 24 or 48 h after transfection with miR-143 and miR-506, at 100 nM, as described above, and stained them with FITC-Annexin V and PI, as previously described (34,35). Subsequently, we analyzed the samples using a BD FACSCalibur Flow Cytometer to determine apoptotic behavior

due to treatment. We measured 10,000 events of the gated population. Untreated cells and cells treated with scrambled siRNA (at 200 nM) with Lipofectamine were used as negative controls.

Cell proliferation. Twenty-four hours after transfection, the cells were seeded in 96-well plates at a density of 2,000 cells per well. Cell proliferation was determined after 48 h, using the reduction of 3-(4,5-dimethylthiazol-2-yl)-2,5-diphenyltetrazolium bromide dye (MTT), according to the manufacture's protocol (Millipore Sigma).

Statistical analysis and database sources. We performed one way analysis of variance (ANOVA) followed by post hoc Tukey's test to determine the significance of differences among groups, unless otherwise specified. We present the mean values ± standard errors; P-values <0.05 were considered statistically significant. We used two database sources to acquire gene expression relevant information in human patients. Data from the Pan-Cancer Analysis, utilizing the ENCORI Platform (http://starbase.sysu.edu.cn/panCancer.php) were used to determine gene expression in human cancer and normal tissues (37,38). Data from Protein Atlas were used to determine survival probability vs. gene expression in patients (http://www.proteinatlas.org; v19.proteinatlas.org) (39,40).

Results

CDK1 and CDK4 are upregulated while miR-143 and miR-506 are downregulated in LC cell lines compared to normal human fetal lung fibroblasts. We quantified the relative gene expression levels of *CDK1* and *CDK4*, using qPCR, in a panel of LC cell lines and compared them to a normal human fetal lung fibroblast cell line, HFL-1. As shown in Fig. 1A and B, both CDK1 and CDK4 expression were significantly higher in all of the tested LC cell lines (P<0.05), compared to HFL-1, except in the case of CDK1 and CDK4 expression in A549 cells and CDK1 expression in H358 cells, which did not achieve significant difference compared to the normal cell line. Specifically, the highest upregulation of CDK1 was in the H69-AR cell line (4.1-fold increase vs. HFL-1; P<0.001), while A549 cells had the lowest levels among the different LC cell lines (1.8-fold increase). In contrast, H358 had the highest levels of CDK4 (4.8-fold increase vs. HFL-1; P<0.05), while A549 also had the lowest levels of CDK4 among the tested cancer cell lines, without achieving significant difference to HFL-1.

Similarly, we quantified the expression of miR-143-3p and miR-506-3p in the LC cell lines, using qPCR, and compared their expression to the normal cell line HFL-1 (Fig. 1C and D). Our analysis indicated a strong and consistent downregulation of miR-143 in the LC cell lines (all P<0.001) compared to HFL-1, which aligns with previous reports (41). In contrast, miR-506 had a variable expression among the different LC cell lines, being significantly lower in A549 (71% downregulation; P<0.001), H69-AR (77% downregulation, P<0.001), H1975 (81% downregulation; P<0.001) and Calu-3 (45% downregulation, P<0.01) compared to the HFL-1 cell line. H358 had approximately similar levels of the gene to HFL-1. Processing data from the Pan-Cancer Analysis, utilizing the ENCORI Platform, we determined the relative expression of CDK1, CDK4, miR-143, and miR-506 genes in lung adenocarcinomas (LUAD) vs. normal tissues (37,38). Briefly, to acquire the relative expression between the LUAD and normal tissue, we used the Starbase website (http://starbase.sysu.edu.cn/panCancer.php) and looked for the relative gene expression by selecting the mRNA or miRNA expression. miR-143-3p was found to be relatively lower in the cancer samples (median: 15.4) compared to the normal samples (median: 18.6; Fig. 1E), while miR-506-3p had low expression but similar levels between cancer (median: -6.6) and normal samples (median: -6.6; Fig. 1F). The expression of CDK1 was higher in the cancer samples (median: 2.7) compared to the normal samples (median: 0.4; Fig. 1G), as well as CDK4 was elevated in the cancer samples (median: 4.4) compared to the normal samples (median: 3.6; Fig. 1H). These data align with our presented analysis of the expression of these genes. Moreover, using the Protein atlas database, we identified a negative correlation between the protein expression for CDK1 and CDK4 vs. median survival in patients with lung adenocarcinomas (Fig. 1I and J).

Combinatorial treatment with miR-143 and miR-506 downregulates the CDK1, CDK4, and CDK6 mRNA and protein expression in cancer cell lines. We transfected the H358 and H1975 cells with the combinatorial treatment of miR-143/506 at 100 nM using Lipofectamine, and analyzed the *CDK1*, *CDK4*, and *CDK6* gene expression, using qPCR at 24 and 48 h post-transfection. The chosen two cell lines carry driver mutations that can complement and correlate with our previously published work on A549 cells (34,35). The treatment downregulated these three genes compared to the untreated or scramble-treated (negative control) groups in both of the cell lines (Fig. 2). In H1975 cells, the combinatorial treatment downregulated the *CDK1, CDK4* and *CDK6* genes by 38% (no significance), 68% (P<0.05) and 63% (P<0.05) at 24 h, respectively, and by 54% (P<0.05), 61% (P<0.05) and 35% (P<0.05) at 48 h, respectively, compared to the untreated control. In H358 cells, the combinatorial treatment downregulated the *CDK1*, *CDK4* and *CDK6* genes by 36% (no significance), 54% (P<0.01) and 27% (no significance) at 24 h, respectively, and by 73% (no significance), 85% (P<0.01), 85% (P<0.01) at 48 h, respectively, compared to the untreated control. Interestingly, in H358 cells, CDK1 was only significantly downregulated when compared to the scramble control at 24 h. Fig. 2 also shows detailed analysis on comparison against the scramble controls.

WB analysis confirmed the downregulation of CDK1 and CDK4 by miR-143/506 transfection. Briefly, the combinatorial treatment significantly reduced the expression levels of both CDK1 and CDK4 proteins after 48 h in both H358 and H1975 cell lines (Fig. 3). Compared to the untreated control at 48 h, we observed a 60% (no significance) and 46% (P<0.05) downregulation of CDK1 and CDK4 genes, respectively, in H358 cells, and a 58% (P<0.01) and 68% (P<0.01) downregulation of CDK1 and CDK4, respectively, in H1975 cells. Compared to scramble treatment at 48 h, we observed a 66% (P<0.05) and 49% (P<0.05) downregulation of CDK1 and CDK4 genes, respectively, in H358 cells, and a 51% (P<0.01) and 77% (P<0.001) downregulation of CDK1 and CDK4, respectively, in H1975 cells. Of note, treatment with scrambled siRNA at

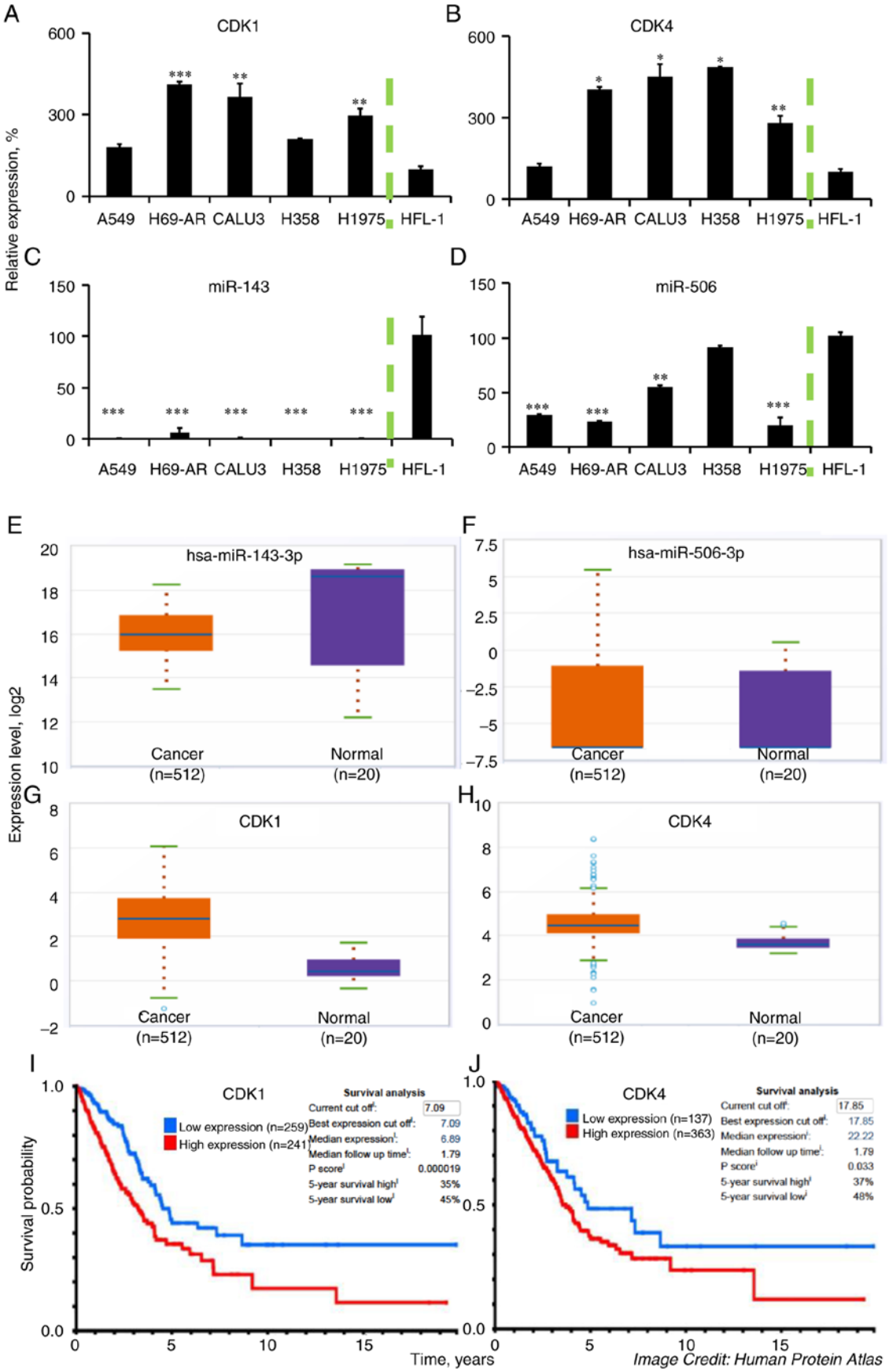

Figure 1. CDK1, CDK4, miR-143, and miR-506 expression in LC cells and LC tissue samples. Higher CDK1 and CDK4 expression levels are associated with poor prognosis in patients with LC adenocarcinomas. We detected the (A) CDK1, (B) CDK4, (C) miR-143, and (D) miR-506, levels in a panel of LC cell lines and compared them to the normal human fetal lung fibroblasts HFL-1, through qPCR. U6 RNA and GAPDH were used as reference genes, where applicable. (E-H) We assessed the relative expression of the same genes in tumor and normal tissues using the ENCORI Pan-Cancer Analysis Platform. (I and J) Kaplan-Meier plots were generated from patient survival using data from the Proteinatlas database (v19.proteinatlas.org/humancell). ***P<0.001; **P<0.01; *P<0.05 compared to HFL-1 cell line. CDK, cyclin-dependent kinase; LC, lung cancer.

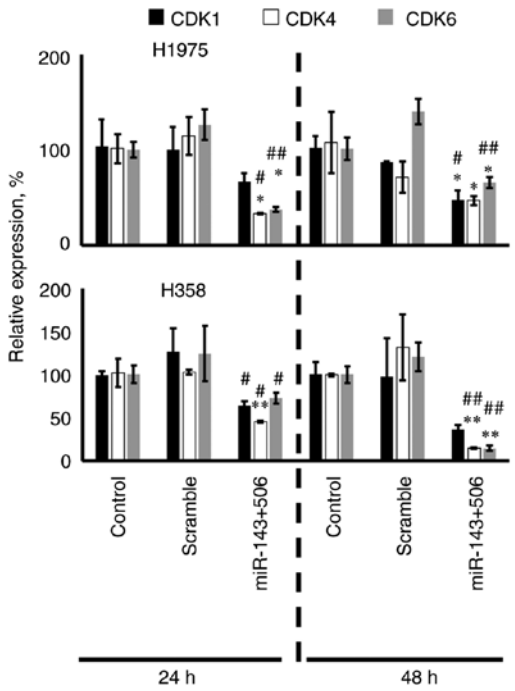

Figure 2. Relative CDK1, CDK4, and CDK6 downregulation following miR-143/506 combinatorial treatment. The analysis of H1975 and H358 LC cells treated with 100 nM miR-143/506 combination using qPCR, for the expression of the 3 CDKs, indicated strong downregulation of the three genes. **P<0.01; *P<0.05 compared to the control; ##P<0.01; #P<0.05 compared to the scramble. CDK, cyclin-dependent kinase; LC, lung cancer.

equimolar concentrations did not significantly alter the expression of the studied genes.

We next evaluated the effect of the individual miRs, as well as their combinatorial treatment in human PC cells (Fig. 4A and B). Forty-eight hours post-transfection with 100 nM miR-143, CDK1 levels were significantly reduced by 66% (P<0.001) in Panc-1 and 44% (P<0.01) in MIA-PaCa-2 cells. miR-143 did not affect CDK4 levels in both of the pancreatic cell lines. Following treatment with equimolar miR-506, CDK4 levels were significantly reduced by 52% (P<0.05) in Panc-1 cells and 57% (P<0.001) in MIA-PaCa-2 cells. Interestingly, miR-506 reduced CDK1 levels by 43% (P<0.001) in Panc-1 cells and 23% (P<0.05) in MIA-PaCa-2 cells. The combination of miR-143 and miR-506 reduced CDK1 levels by 70 and 88% (P<0.001 for both) in Panc-1 and MIA-PaCa-2 cells, respectively. Moreover, the combinatorial miR treatment reduced CDK4 levels by 58% (P<0.05) and 56% (P<0.001) in Panc-1 and MIA-PaCa-2 cells, respectively.

miR-143 and miR-506 combinatorial treatment increased the G_0/G_1 and G_2 cell populations. We evaluated the cell cycle regulatory effect of miR-143/506 combination using flow cytometry in H1975 and H358 cell lines. We transfected the cells, as described above, and performed the PI staining method to analyze the cell cycle phase of the cells. For comparison, we utilized two cell cycle inhibitors, ribociclib at 3 μM (42,43) and flavopiridol at 100 nM (44,45). Ribociclib is an FDA-approved, clinically used CDK4/6 inhibitor, and flavopiridol is a clinically tested CDK1, CDK2, CDK4, and CDK7 inhibitor (43,44,46).

Our analysis on H358 cells indicated that the combinatorial treatment significantly increased the G_0/G_1 cell population (53.5 and 63%; all values in parenthesis indicate the percent of the specific population to the total) compared to the untreated (46 and 44%; P<0.001) and scramble (49.5 and 45.5%; P<0.001) control groups, at both 24 and 48 h, respectively. Interestingly, ribociclib more robustly increased the G_0/G_1 cell population (70.5%; P<0.001) at 24 h compared to the miR treatment. In contrast, ribociclib had significantly lower G_0/G_1 cell population (52%; P<0.01) at 48 h compared to the miR treatment, which indicates a potentially prolonged inhibition of the cell cycle progression due to the miR treatment compared to ribociclib. Flavopiridol decreased the G_0/G_1 phase population (42.5%; P<0.05) at 24 h, while it increased the G_0/G_1 population (52%; P<0.05) at 48 h, compared to untreated control. However, in both time points, the combinatorial treatment more potently increased the G_0/G_1 populations compared to flavopiridol (P<0.01). The combinatorial treatment did not alter the cell population at the S phase (26%), compared to the control (29.5%; no significance) at 24 h, but decreased the S phase population (13%) compared to the control (39.5%; P<0.01) at 48 h. Ribociclib treatment decreased the cell population in the S phase (14%; P<0.01), compared to the untreated control at 24 h, while the decrease in the S phase population was less potent (28%; P<0.01) at 48 h. In contrast, flavopiridol modestly increased the S phase population (38%) compared to the untreated (no significance) at 24 h, and lowered the S phase population (25.5%; P<0.05) compared to the untreated control group at 48 h. No significant changes were observed for any treatment for both time points at the G_2 cell populations, with the exception of ribociclib reducing the G_2 population (15.5%) compared to the untreated control (24.5%, P<0.05) at 24 h (Fig. 5).

Our analysis on H1975 indicated that the combinatorial miR treatment increased the G_0/G_1 phase cell population (60 and 57%) compared to the untreated control (46 and 54%) at 24 (P<0.001) and 48 h (no significance), respectively. In comparison to the scramble control though, a significant increase in the G_0/G_1 was observed for the combinatorial miR treatment for both time points (P<0.001). Unlike H358 cells, we did not observe any significant increase in the G_0/G_1 phase population due to ribociclib treatment (61%; no significance) compared to the combinatorial treatment at 24 h, though this was higher (64%; P<0.05) at 48 h. In both time points, ribociclib increased the G_0/G_1 cell population compared to untreated control (P<0.01). Flavopiridol did not produce a significant difference compared to the combinatorial miR treatment at the G_0/G_1 phase cell populations (60 and 59% at 24 and 48 h, respectively). However, it was higher compared to the untreated controls (P<0.05), at both 24 and 48 h. The combinatorial treatment reduced the S phase population at 24 h (21%) compared to the untreated (42%; P<0.001) and scramble controls (38%; P<0.01). In contrast, the combinatorial treatment did not alter the S phase population (28%) compared to the untreated control (33%; no significance) at 48 h, but lowered the S phase population compared to the scramble control (40%; P<0.01). The combinatorial miR treatment more potently reduced the S phase population compared to ribocliclib (29%; P<0.05) at 24 h, but ribociclib more potently reduced the S phase population (17%) compared to the combinatorial miR treatment

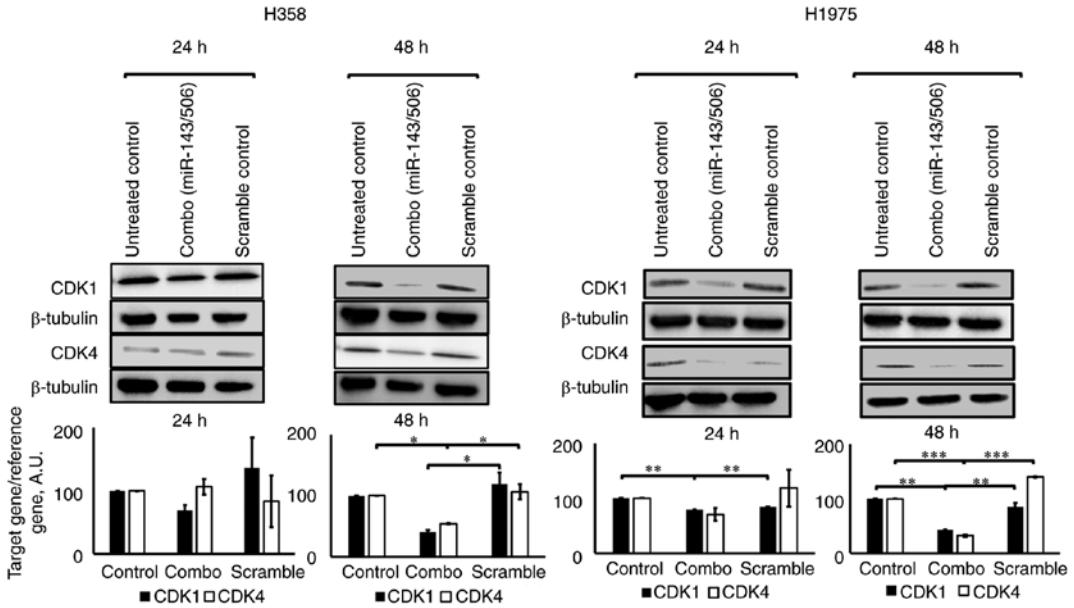

Figure 3. Western blot (WB) analysis of CDK1 and CDK4 protein downregulation following transfection with the combinatorial miR-143/506 treatment. Upper panel: WB analysis confirmed the downregulation of the CDK1 and CDK4 genes due to the combinatorial miR treatment at 100 nM at the post-transcriptional level. Negative controls include untreated cells and cells treated with equimolar scramble siRNA. Lower panel: Semi-quantitative histogram analysis of the WBs. ***P<0.001; **P<0.01; *P<0.05 compared to the control. CDK, cyclin-dependent kinase.

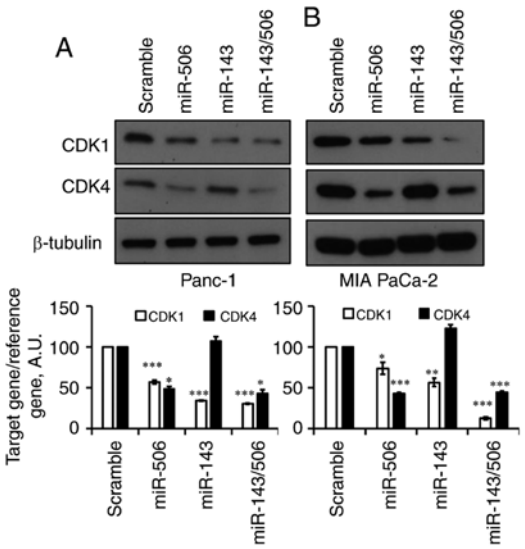

Figure 4. miR-143 and miR-506 transfection downregulates CDK expression. The combinatorial miR treatment at 100 nM downregulated CDK1 and CDK4 protein expressions at 48 h in (A) PC Panc-1 and (B) MIA-Paca-2 cells. ***P<0.001; **P<0.01; *P<0.05 compared to the control. CDK, cyclin-dependent kinase; PC, pancreatic cancer.

(28%; P<0.01) at 48 h. For both time points, flavopiridol did not demonstrate significant differences compared to the combinatorial treatment. Both CDK-inhibitors decreased the S phase populations significantly compared to the respective untreated controls for both time points. Finally, at 24 h, the combinatorial miR treatment increased the G_2 phase population (18.5%) compared to the untreated control (13%; P<0.05), scramble control (12%; P<0.05), which was similar to flavopiridol (21%; no significance compared to combinatorial treatment) and significantly higher compared to ribociclib (10%; P<0.05 compared to combinatorial miR treatment; Fig. 5). At 48 h, no significant differences were observed among any of the groups. Detailed data on the cell cycle cell distributions are presented in Table I.

The miR-143/506 combination induces apoptotic activity in LC cells, but has a lesser effect on normal lung fibroblasts, and reduces PC cell growth. We investigated the capacity of the combinatorial miR-143 and miR-506 treatment to induce apoptosis in H358 and H1975 LC cell lines, as well as in the normal human fetal lung fibroblast HFL-1 cells, using flow cytometry and Annexin V/PI (Fig. 6). Our analysis indicated that the combinatorial miR-143/506 treatment strongly induced apoptosis in both LC cell lines. In contrast, the apoptotic activity in the normal cell line was more modest and peaked at 24 h. Detailed information for all cell populations is documented in Table SII, as here we focus on the late apoptotic and necrotic populations.

Briefly, in the H358 cells and at 24 h, the combinatorial miR treatment increased (33%) the late apoptotic and necrotic cell populations compared to the untreated (11%, P<0.001) and the scramble controls (14.63%, P<0.01). At 48 h, the miR-143/506 treatment induced more potent apoptotic activity, where the majority of the cells were in the late apoptotic and necrotic populations (50%) compared to the untreated control (10%; P<0.01) and the scramble control (24%; P<0.05).

Comparably, in the H1975 cells and at 24 h, our analysis indicated that the combinatorial treatment induced an increase in the late apoptotic and necrotic populations (69%) compared to the untreated control (17%; P<0.001) and scramble control (18%; P<0.001). At 48 h, the observed apoptotic activity of the combinatorial treatment was maintained, as the combinatorial treatment significantly increased the late apoptosis and necrotic cell populations (57%) compared to the untreated control (9%; P<0.001) and scramble treated control (18%; P<0.01).

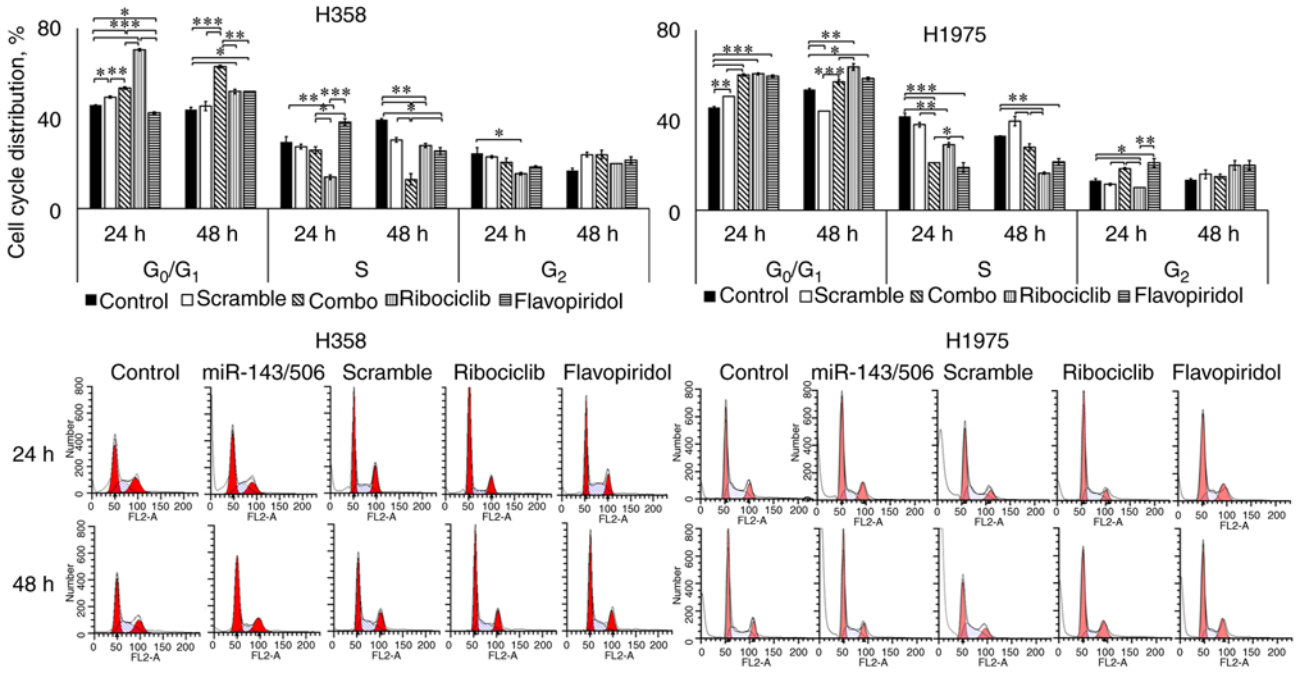

Figure 5. Cell cycle analysis of LC cells treated with miR-143/506 combination indicates a behavior comparable to clinically used cell cycle inhibitors, ribociclib, and flavopiridol. Upper panel: Cell cycle analysis of H358 and H1975 cells to identify cell populations according to their observed cell cycle progression, following treatment with miR-143/506 at 100 nM using lipofectamine (Combo), ribociclib at 3 μM and flavopiridol at 100 nM. Untreated cells (Control) and cells treated with equimolar scramble siRNA in Lipofectamine (Scramble) were used as negative controls. Lower panel: Representative histograms from flow cytometric analysis. ***P<0.001; **P<0.01; *P<0.05. LC, lung cancer.

In the normal HFL-1 cell line and at 24 h, we detected an increase in late apoptotic and necrotic populations due to the combinatorial treatment (28%) compared to the untreated control (9%; P<0.05) and compared to the scramble control (9%; P<0.05). At 48 h, we observed an increase in late apoptotic and necrotic populations due to the combinatorial miR treatment (16%) compared to the untreated control (1%; P<0.05) and to scramble treatment (1%; P<0.05).

Finally, we performed a cytotoxicity analysis of miR-143 and miR-506 treatment, individually and in combination in Panc-1 and MIA-PaCa-2 cells, for 48 h (Fig. 7). We observed a significant (P<0.001) reduction of viable Panc-1 (85%) and MIA-PaCa-2 (72%) cells, due to the combinatorial miR treatment. The cytotoxic effect of the combinatorial miR treatment was also significantly stronger (P<0.001) when compared to the individual miR-143 or miR-506 in Panc-1 cells. Briefly, we observed a significant reduction in viable cells in both PC cell lines due to treatment with the individual miRs compared to the untreated (P<0.01) and scramble (P<0.05) controls. At 48 h post-transfection, miR-143 reduced by 60 and 50% the viable cell population in Panc-1 and MIA-PaCa-2 cells, respectively, whereas miR-506 reduced by 58 and 49% the cell population in Panc-1 and MIA-PaCa-2 cell lines, respectively (all values had at least P<0.05).

Discussion

MicroRNAs (miRNAs/miRs) are critical regulators of mRNA expression, and various diseases, including cancer, have been associated with miR dysregulation (47,48). We recently reported on two miRs, miR-143 and miR-506, previously recognized with essential functions in cancer and other diseases (34,35,49,50). miR-143 has base-pair complementarity with the 3'-UTR region of cyclin-dependent kinase 1 (CDK1), and miR-506 has base-pair complementarity with the 3'-UTR regions of CDK4 and CDK6 (35,51,52). The data presented here support the notion that the combinatorial miR treatment has a potent cell cycle inhibiting capacity in two cell cycle phase transitions, through the downregulation of CDKs. This represents a promising therapeutic option for cancers in which CDK4/6 monotherapy is unlikely to exert sufficient therapeutic outcomes, such as in lung cancer (LC) and pancreatic cancer (PC).

Initially, we determined the expression of miR-143 and miR-506 in LC cells. Expression of the two miRs were found to be lower in LC cell lines compared to a normal human fetal lung fibroblast cell line (HFL-1). Although not all cancer cell lines showed a significant miR-506 expression difference compared to normal cell lines, our data align with previously reported analyses showing a dysregulation of miR-143/506 in LC cells vs. normal cells (41,53). Interestingly, *CDK1* and *CDK4* gene expression levels were significantly higher in all of the LC cell lines tested compared to HLF-1, with the exception of A549 for *CDK1* and *CDK4* and H358 for *CDK1*. Of interest, H358 showed increased CDK4 expression, without a significant miR-506 downregulation. This indicates potentially that even though miR-506 can regulate CDK4 expression, it is not its sole regulator. Furthermore, as the miR-506 expression levels in normal or cancer cells were found to be very low (as presented by the tissue samples and Pan-Cancer analysis), exogenous overexpression of miR-506 could potentially have more potent effect than its basal expression changes on CDK4 expression. Briefly, we used data from the Pan-Cancer Analysis to determine the differential expression of the above

Table I. Detailed data of cell cycle distribution depending on cell cycle phases for H358 and H1975 cells following treatment with miR-143/506, ribociclib or flavopiridol.

	H358 cell line					
	G_0/G_1		S		G_2	
Avg ± SEM	24 h	48 h	24 h	48 h	24 h	48 h
Control	46±0	44±1	29.5±2.5	39.5±0.5	24.5±2.5	17±1
Scramble	49.5±0.5	45.5±2	27.5±1	30.5±1	23±0.5	24±1
Combo	53.5±0.5	63±0.5	26±1.5	13±2.5	20.5±2	24±2
Ribociclib	70.5±0.5	52±1	14±1	28±1	15.5±0.5	20±0
Flavopiridol	42.5±0.5	52±0	38.5±1.5	25.5±1.5	18.5±0.5	21.5±1.5
	G_0/G_1		S		G_2	
Tukey's test vs. control group	24 h	48 h	24 h	48 h	24 h	48 h
Scramble	<0.05	>0.05	>0.05	<0.05	>0.05	>0.05
Combo	<0.001	<0.001	>0.05	<0.001	>0.05	>0.05
Ribociclib	<0.001	<0.05	<0.01	<0.05	<0.05	>0.05
Flavopiridol	<0.05	<0.05	>0.05	<0.05	>0.05	>0.05
	H1975 cell line					
	G_0/G_1		S		G_2	
Avg ± SEM	24 h	48 h	24 h	48 h	24 h	48 h
Control	45.5±0.5	53.5±0.5	41.5±1.5	33±0	13±1	13.5±0.5
Scramble	50.5±0	44±0	38±1	39.5±2	11.5±0.5	16±2
Combo	60±0.5	57±1	21±0	28±1.5	18.5±0.5	15±1
Ribociclib	60.5±0.5	63.5±1.5	29±1	16.5±0.5	10±0	20±2
Flavopiridol	59.5±0.5	58.5±0.5	19±2	21.5±1.5	21±2	20±2
	G_0/G_1		S		G_2	
Tukey's test vs. control group	24 h	48 h	24 h	48 h	24 h	48 h
Scramble	<0.01	<0.01	>0.05	>0.05	>0.05	>0.05
Combo	<0.001	>0.05	<0.001	>0.05	>0.05	>0.05
Ribociclib	<0.001	<0.01	<0.01	<0.01	>0.05	>0.05
Flavopiridol	<0.001	<0.05	<0.001	<0.01	<0.05	>0.05

All statistical analyses were conducted using one-way ANOVA followed by Tukey's test.

genes in tumor tissues from patients with lung adenocarcinomas compared to normal tissues. Consistent with our findings, miR-143-3p was lower in cancer vs. normal samples. Interestingly, miR-506-3p was expressed relatively low in tumor and normal tissue samples, without a difference between the two sample groups. Finally, both CDK1 and CDK4 were higher in cancer samples compared to normal samples, and more importantly, protein expression for CDK1 and CDK4 vs. survival in patients with LC adenocarcinomas indicated a negative correlation between CDK1 and CDK4 expression and survival. We recently reported that miR-143 and miR-506 have CDK1 and CDK4 mRNAs as their predicted targets, respectively (34,35). These data align with previously reported work on these genes (13,32). Here, our analysis of the miR-143/506 combination on H358, and H1975 LC cell lines, confirmed our previous findings on CDK1, CDK4 and CDK6 downregulation (34,35). The downregulation of these genes took place at both the post-transcriptional and translational level. We selected the two cell lines for analysis, as they carry driver mutations that complement or correlate with our previously published work on A549 cells, as we further analyze below. This analysis correlates also with the reported activity of miR-143 or miR-506 alone (35,51,54). Interestingly, although the combinatorial miR treatment downregulated CDK1 in H358 cells, the downregulation achieved statistical significance only for the 24 h time point, compared to the scramble control. An important feature of our study is that the combinatorial treatment inhibited the cell cycle progression in the H358 and H1975 cells, comparably to clinically used cell cycle inhibitors. Specifically, we used as positive controls two cell cycle inhibitors, ribociclib and flavopiridol, which the former is currently clinically used for breast cancer treatment, and the latter has been evaluated in clinical trials. Flavopiridol inhibits the activity of the CDK1/2/4/7, and causes cell cycle halt at the

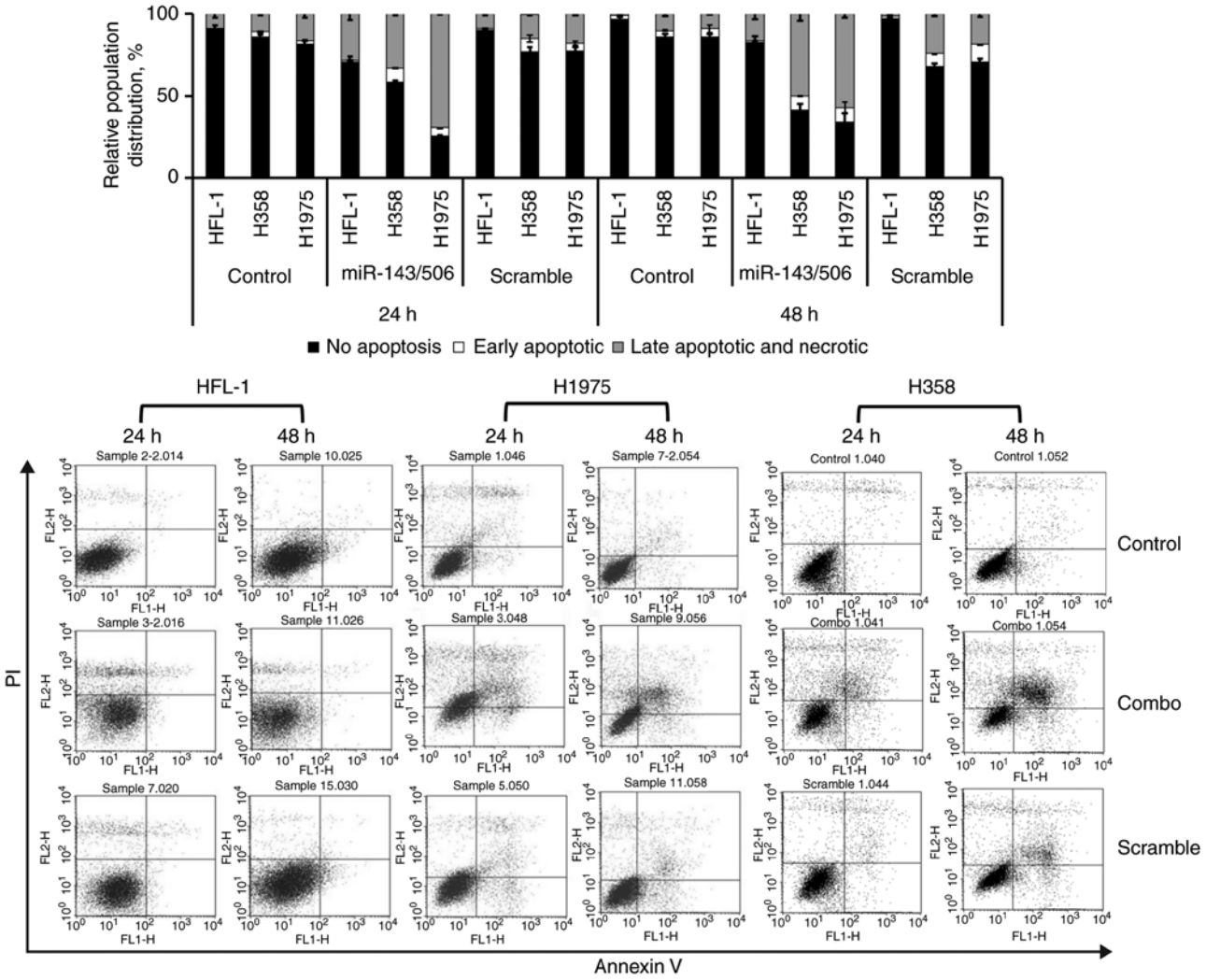

Figure 6. Apoptosis analysis of LC cells compared to normal lung fibroblasts indicates a stronger effect in the tumor cells. Annexin V/PI apoptosis analysis of HFL-1, H358, and H1975 cell populations, as determined by flow cytometric quantification, at 24 and 48 h post-transfection, and representative scatter graphs. LC, lung cancer.

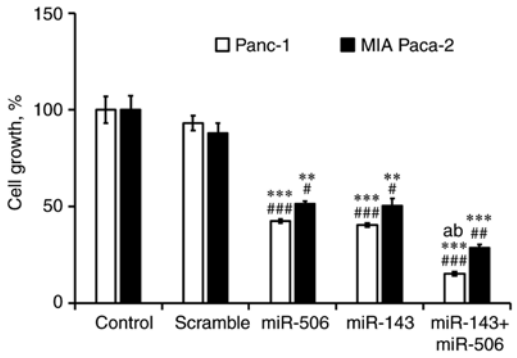

Figure 7. miR-143 and miR-506 transfection is cytotoxic in human PC cells. Cell growth determined by MTT assay in Panc-1 and MIA PaCa-2 cells treated with miR143, miR506, or both for 48 h. ***P<0.001 and **P<0.01 vs. the control group; $^{###}$P<0.001, $^{##}$P<0.01 and $^{#}$P<0.05 vs. the scramble; ^{a}P<0.001 vs. miR-506; ^{b}P<0.001 vs. miR-143. PC, pancreatic cancer.

G_1/S and G_2/M transitions (55,56) and ribociclib (LEE011) is a selective CDK4/6 inhibitor, halting cell cycle progression at the G_1/S transition (3,12). Flow-cytometric analysis indicated a significant increase in the G_0/G_1 cell populations due to the combinatorial miR treatment in both cell lines at either 24 or 48 h post-transfection. The combinatorial miR treatment's increase of the G_0/G_1 population was comparable to, and, in some cases, higher than either ribociclib or flavopiridol. In contrast, the combinatorial miR treatment significantly decreased the cell population in the S phase compared to the untreated and scramble controls, comparably to the two cell cycle inhibitors, albeit at different time points in some cases. These results suggest that the miR-143/506 treatment potentiates an inhibition of the G_1/S transition progression, and is comparable to the activity of the G_1/S cell cycle inhibitors.

The combinatorial miR treatment increased the G_2 cell population in both cell lines compared to the untreated cells, though the increase was significant only in the H1975 when compared to the untreated and scramble group. The increase in the G_2 cell population due to miR treatment was similar to the effect of flavopiridol in the same cell population for both cell lines, which is considered a G_2/M inhibitor. In contrast, ribociclib, which does not inhibit G_2/M transition, did not increase the G_2 population. This indicates that the miR-143/506 treatment can induce a two phase transition inhibition, i.e., at both G_1/S and a G_2/M transitions, in LC cells. Interestingly,

the G_2/M inhibition activity for both miR-143/506 combination and flavopiridol was more potent in the H1975 cells, while modest in H358. This potentially could be attributed to a potential different molecular mechanism, as the two cell lines carry different driver mutations. There is a correlation between the activities of the combinatorial miR treatment and flavopiridol, the G_1/S and G_2/M inhibitor. Though both treatments induced a significant increase of the G_2 cell populations in H1975, this was not observed in H358. In fact, this observation also correlates with the inability of the combinatorial miR treatment to significantly downregulate the CDK1 expression in the H358 cells. These results reinforce the notion that the miR-treatment correlates with a G_1/S and G_2/M inhibitor, albeit the mutational background of each cell line needs to be taken into consideration. Briefly, H358 cells carry a mutated *KRAS* and have an inactive (deleted) *TP53* gene, while H1975 have a wt-*KRAS*, and mutated *CDKN2A*, *PIK3CA*, *TP53* and *EGFR* genes (57-59). Our work compares and expands to our previously presented data on A549 cells, which carry wt-*p53*, mutated *KRAS* and mutated *CDKN2A*. Our results merit future analyses based on the different driver mutations, as they will assist in identifying the mechanistic background on the activity of the combinatorial miR treatment.

Subsequently, we evaluated the apoptotic activity of the combinatorial miR treatment in LC cell lines and compared them to HFL-1 normal human fetal lung fibroblasts. We observed a significant apoptotic activity in the LC cells, due to the combinatorial miR treatment, at 24 and 48 h post-transfection. Interestingly, the combinatorial miR treatment had a modest apoptotic effect in the HFL-1 cell line. Briefly, the combinatorial miR treatment induced apoptotic activity in HFL-1 cells that was less potent when compared to the H358 and H1975 cells ($P<0.05$ for both cell lines) at 24 h, and was practically normalized at 48 h. In contrast, the apoptotic activity of the miR treatment remained potent in the H1975 cell at both 24 and 48 h, while in H358 cells, the miR treatment induced a modest apoptotic activity at 24 h, but became more robust and comparable to H1975 cells at 48 h. This behavior difference between the two LC cell lines correlates to the observed activity of the miR treatment on the cell cycle analysis, where the strongest decrease in the S population and strongest increase of the G_2 population was observed at 24 h for the H1975 and 48 h for the H358. The modest apoptotic activity of the combinatorial treatment in the HFL-1 cells could potentially be justified by the relative higher expression of these miRs in this normal cell line compared to the cancer cells, and can potentially indicate a preferential activity against tumor cells vs. normal cells. This could potentially translate to decreased side effects (i.e., toxicity to normal cells) if the combination miR therapy is clinically translated.

Having established the capacity of the two miRs to downregulate the CDKs in LC cells and induce apoptosis, we determined whether the effects were cancer-type specific. Though significant differences exist between PC and LC cells, mutations in similar genes have been detected in the both cancer types (60,61). For example, both Panc-1 and MIA-PacCa-2 cell lines carry mutated or deleted *TP53*, *CDKN2A*, and *KRAS* genes, partially similar to either H358 or H1975. Thus, the genetic background similarities prompted us to expand to the PC cells and use Panc-1 and MIA-PaCa-2 cell lines as proof-of-concept. We confirmed our findings in these two PC cell lines that the two miRs downregulated CDK1 and CDK4 expression and induced cytotoxicity (62). Similar to the LC cells, the miR-143/506 treatment strongly downregulated both CDK1 and CDK4 protein expression. Furthermore, the individual miR treatment specifically downregulated their respective target, i.e., miR-143 downregulated CDK1 and miR-506 downregulated mostly CDK4. This led to a significant reduction in PC cell growth, with the combination treatment being substantially more potent that the individual miR treatments. These results are in agreement with our previous analysis of the individual miRs on the A549 LC cells (35), and indicate that the two miRs have an activity that spans outside a specific cancer type.

Our data presented here, as well as in our previous studies, reaffirm that the combinatorial miR treatment have a potent cell cycle inhibiting capacity in two phase transitions, through the downregulation of CDKs, comparable to respective CDK inhibitors. This represents a promising therapeutic option for cancers that CDK4/6 monotherapy is unlikely to exert sufficient therapeutic outcomes. The combinatorial miR treatment acts in both LC and PC, which presents a non-cancer-type specific therapeutic benefit for potential cancer treatment.

In conclusion, the combinatorial miR-143 and miR-506 therapy, through the downregulation of CDK1, CDK4 and CDK6, strongly inhibits the cell cycle progression to a comparable degree as the clinically used CDK-inhibitor ribociclib and the clinically evaluated CDK-inhibitor flavopiridol. In addition, the miR-143/506 combinatorial treatment selectively induces apoptotic activity in the LC cells, with comparably diminished effect on normal fibroblast cells. Finally, this combination of miR treatment is effective in PC cells, suggesting a broader application for the miR-143/506 combinatorial treatment. Overall, these data support the notion that the miR-143/506 combinatorial treatment is a promising approach for regulating the cell cycle progression that merits further evaluation.

Acknowledgements

Not applicable.

Funding

This work was supported by the College of Pharmacy, University of Louisiana Monroe start-up funding, and the National Institutes of Health (NIH) through the National Institute of General Medical Science Grants 5 P20 GM103424-15, 3 P20 GM103424-15S1.

Availability of data and materials

All data generated or analyzed during this study are included in this published article.

Authors' contributions

AKMNH collected, analyzed and interpreted the data regarding the LC cell lines, and was a major contributor in writing the manuscript. GGM collected, analyzed and interpreted the data

regarding the PC cell lines, and was a contributor in writing the manuscript. GM analyzed and interpreted the data, and was a major contributor in writing the manuscript. All authors read and approved the final manuscript.

Ethics approval and consent to participate

Not applicable.

Patient consent for publication

Not applicable.

Competing interests

The authors have no competing interests to report.

References

1. Siegel RL, Miller KD and Jemal A: Cancer statistics, 2020. CA Cancer J Clin 70: 7-30, 2020.
2. Collins K, Jacks T and Pavletich NP: The cell cycle and cancer. Proc Natl Acad Sci USA 94: 2776-2778, 1997.
3. Dominguez-Brauer C, Thu KL, Mason JM, Blaser H, Bray MR and Mak TW: Targeting Mitosis in cancer: Emerging strategies. Mol Cell 60: 524-536, 2015.
4. Otto T and Sicinski P: Cell cycle proteins as promising targets in cancer therapy. Nat Rev Cancer 17: 93-115, 2017.
5. Kastan MB and Bartek J: Cell-cycle checkpoints and cancer. Nature 432: 316-323, 2004.
6. Sanchez-Martinez C, Gelbert LM, Lallena MJ and de Dios A: Cyclin dependent kinase (CDK) inhibitors as anticancer drugs. Bioorg Med Chem Lett 25: 3420-3435, 2015.
7. Shah A, Bloomquist E, Tang S, Fu W, Bi Y, Liu Q, Yu J, Zhao P, Palmby TR, Goldberg KB, *et al*: FDA approval: Ribociclib for the treatment of postmenopausal women with hormone receptor-positive, HER2-negative advanced or metastatic breast cancer. Clin Cancer Res 24: 2999-3004, 2018.
8. Asghar U, Witkiewicz AK, Turner NC and Knudsen ES: The history and future of targeting cyclin-dependent kinases in cancer therapy. Nat Rev Drug Discov 14: 130-146, 2015.
9. Wedam S, Fashoyin-Aje L, Bloomquist E, Tang S, Sridhara R, Goldberg KB, Theoret MR, Amiri-Kordestani L, Pazdur R and Beaver JA: FDA approval summary: Palbociclib for male patients with metastatic breast cancer. Clin Cancer Res 26: 1208-1212, 2020.
10. FDA expands approved use of ibrance (Palbociclib) for HR+, HER2-metastatic breast cancer. Oncol Times 38: 22, 2016.
11. Martin JM and Goldstein LJ: Profile of abemaciclib and its potential in the treatment of breast cancer. Onco Targets Ther 11: 5253-5259, 2018.
12. Jin D, Tran N, Thomas N and Tran DD: Combining CDK4/6 inhibitors ribociclib and palbociclib with cytotoxic agents does not enhance cytotoxicity. PLoS One 14: e0223555, 2019.
13. Wu A, Wu B, Guo J, Luo W, Wu D, Yang H, Zhen Y, Yu X, Wang H, Zhou Y, *et al*: Elevated expression of CDK4 in lung cancer. J Transl Med 9: 38, 2011.
14. Gong W, Wang L, Zheng Z, Chen W, Du P and Zhao H: Cyclin-dependent kinase 6 (CDK6) is a candidate diagnostic biomarker for early non-small cell lung cancer. Transl Cancer Res 9: 95-103, 2019.
15. Thangavel C, Boopathi E, Liu Y, McNair C, Haber A, Perepelyuk M, Bhardwaj A, Addya S, Ertel A, Shoyele S, *et al*: Therapeutic challenge with a CDK 4/6 Inhibitor Induces an RB-Dependent SMAC-Mediated apoptotic response in non-small cell lung cancer. Clin Cancer Res 24: 1402-1414, 2018.
16. Patnaik A, Rosen LS, Tolaney SM, Tolcher AW, Goldman JW, Gandhi L, Papadopoulos KP, Beeram M, Rasco DW, Hilton JF, *et al*: Efficacy and safety of abemaciclib, an inhibitor of CDK4 and CDK6, for patients with breast cancer, non-small cell lung cancer, and other solid tumors. Cancer Discov 6: 740-753, 2016.
17. Pacheco J and Schenk E: CDK4/6 inhibition alone and in combination for non-small cell lung cancer. Oncotarget 10: 618-619, 2019.
18. Waddell N, Pajic M, Patch AM, Chang DK, Kassahn KS, Bailey P, Johns AL, Miller D, Nones K, Quek K, *et al*: Whole genomes redefine the mutational landscape of pancreatic cancer. Nature 518: 495-501, 2015.
19. Witkiewicz AK, McMillan EA, Balaji U, Baek G, Lin WC, Mansour J, Mollaee M, Wagner KU, Koduru P, Yopp A, *et al*: Whole-exome sequencing of pancreatic cancer defines genetic diversity and therapeutic targets. Nat Commun 6: 6744, 2015.
20. Serrano M, Lin AW, McCurrach ME, Beach D and Lowe SW: Oncogenic ras provokes premature cell senescence associated with accumulation of p53 and p16INK4a. Cell 88: 593-602, 1997.
21. Weinberg F, Hamanaka R, Wheaton WW, Weinberg S, Joseph J, Lopez M, Kalyanaraman B, Mutlu GM, Budinger GR and Chandel NS: Mitochondrial metabolism and ROS generation are essential for Kras-mediated tumorigenicity. Proc Natl Acad Sci USA 107: 8788-8793, 2010.
22. Garcia-Reyes B, Kretz AL, Ruff JP, von Karstedt S, Hillenbrand A, Knippschild U, Henne-Bruns D and Lemke J: The emerging role of cyclin-dependent kinases (CDKs) in pancreatic ductal adenocarcinoma. Int J Mol Sci 19: 3219, 2018.
23. Knudsen ES, Kumarasamy V, Ruiz A, Sivinski J, Chung S, Grant A, Vail P, Chauhan SS, Jie T, Riall TS and Witkiewicz AK: Cell cycle plasticity driven by MTOR signaling: Integral resistance to CDK4/6 inhibition in patient-derived models of pancreatic cancer. Oncogene 38: 3355-3370, 2019.
24. Franco J, Balaji U, Freinkman E, Witkiewicz AK and Knudsen ES: Metabolic reprogramming of pancreatic cancer mediated by CDK4/6 inhibition elicits unique vulnerabilities. Cell Rep 14: 979-990, 2016.
25. Liu F and Korc M: Cdk4/6 inhibition induces epithelial-mesenchymal transition and enhances invasiveness in pancreatic cancer cells. Mol Cancer Ther 11: 2138-2148, 2012.
26. Franco J, Witkiewicz AK and Knudsen ES: CDK4/6 inhibitors have potent activity in combination with pathway selective therapeutic agents in models of pancreatic cancer. Oncotarget 5: 6512-6525, 2014.
27. Santamaria D, Barriere C, Cerqueira A, Hunt S, Tardy C, Newton K, Cáceres JF, Dubus P, Malumbres M and Barbacid M: Cdk1 is sufficient to drive the mammalian cell cycle. Nature 448: 811-815, 2007.
28. Malumbres M, Sotillo R, Santamaria D, Galán J, Cerezo A, Ortega S, Dubus P and Barbacid M: Mammalian cells cycle without the D-type cyclin-dependent kinases Cdk4 and Cdk6. Cell 118: 493-504, 2004.
29. Piao J, Zhu L, Sun J, Li N, Dong B, Yang Y and Chen L: High expression of CDK1 and BUB1 predicts poor prognosis of pancreatic ductal adenocarcinoma. Gene 701: 15-22, 2019.
30. Dong S, Huang F, Zhang H and Chen Q: Overexpression of BUB1B, CCNA2, CDC20, and CDK1 in tumor tissues predicts poor survival in pancreatic ductal adenocarcinoma. Biosci Rep 39: BSR20182306, 2019.
31. Shi YX, Zhu T, Zou T, Zhuo W, Chen YX, Huang MS, Zheng W, Wang CJ, Li X, Mao XY, *et al*: Prognostic and predictive values of CDK1 and MAD2L1 in lung adenocarcinoma. Oncotarget 7: 85235-85243, 2016.
32. Li M, He F, Zhang Z, Xiang Z and Hu D: CDK1 serves as a potential prognostic biomarker and target for lung cancer. J Int Med Res 48: 300060519897508, 2020.
33. O'Brien J, Hayder H, Zayed Y and Peng C: Overview of MicroRNA biogenesis, mechanisms of actions, and circulation. Front Endocrinol (Lausanne) 9: 402, 2018.
34. Hossian AK, Muthumula CM, Sajib MS, Tullar PE, Stelly AM, Briski KP, Mikelis CM and Matthaiolampakis G: Analysis of combinatorial miRNA treatments to regulate cell cycle and angiogenesis. J Vis Ex: e59460, 2019.
35. Hossian AKMN, Sajib MS, Tullar PE, Mikelis CM and Mattheolabakis G: Multipronged activity of combinatorial miR-143 and miR-506 inhibits lung cancer cell cycle progression and angiogenesis in vitro. Sci Rep 8: 10495, 2018.
36. Livak KJ and Schmittgen TD: Analysis of relative gene expression data using real-time quantitative PCR and the 2(-Delta Delta C(T)) method. Methods 25: 402-408, 2001.
37. Li JH, Liu S, Zhou H, Qu LH and Yang JH: StarBase v2.0: Decoding miRNA-ceRNA, miRNA-ncRNA and protein-RNA interaction networks from large-scale CLIP-Seq data. Nucleic Acids Res 42: D92-D97, 2014.
38. Yang JH, Li JH, Shao P, Zhou H, Chen YQ and Qu LH: StarBase: A database for exploring microRNA-mRNA interaction maps from Argonaute CLIP-Seq and degradome-Seq data. Nucleic Acids Res 39: D202-D209, 2011.

39. Thul PJ and Lindskog C: The human protein atlas: A spatial map of the human proteome. Protein Sci 27: 233-244, 2018.
40. Uhlen M, Fagerberg L, Hallstrom BM, Lindskog C, Oksvold P, Mardinoglu A, Sivertsson Å, Kampf C, Sjöstedt E, Asplund A, *et al*: Proteomics. Tissue-based map of the human proteome. Science 347: 1260419, 2015.
41. Zhang N, Su Y and Xu L: Targeting PKCε by miR-143 regulates cell apoptosis in lung cancer. FEBS Lett 587: 3661-3667, 2013.
42. van Caloen G, Schmitz S, El Baroudi M, Caignet X, Pyr Dit Ruys S, Roger PP, Vertommen D and Machiels JP: Preclinical activity of ribociclib in squamous cell carcinoma of the head and neck. Mol Cancer Ther 19: 777-789, 2020.
43. Wong CH, Ma BB, Hui CW, Lo KW, Hui EP and Chan AT: Preclinical evaluation of ribociclib and its synergistic effect in combination with alpelisib in non-keratinizing nasopharyngeal carcinoma. Sci Rep 8: 8010, 2018.
44. Kelland LR: Flavopiridol, the first cyclin-dependent kinase inhibitor to enter the clinic: Current status. Expert Opin Investig Drugs 9: 2903-2911, 2000.
45. Saisomboon S, Kariya R, Vaeteewoottacharn K, Wongkham S, Sawanyawisuth K and Okada S: Antitumor effects of flavopiridol, a cyclin-dependent kinase inhibitor, on human cholangiocarcinoma in vitro and in an in vivo xenograft model. Heliyon 5: e01675, 2019.
46. Senderowicz AM and Sausville EA: Preclinical and clinical development of cyclin-dependent kinase modulators. J Natl Cancer Inst 92: 376-387, 2000.
47. Hossian AKMN, Mackenzie GG and Mattheolabakis G: miRNAs in gastrointestinal diseases: Can we effectively deliver RNA-based therapeutics orally? Nanomedicine (Lond) 14: 2873-2889, 2019.
48. Labatut AE and Mattheolabakis G: Non-viral based miR delivery and recent developments. Eur J Pharm Biopharm 128: 82-90, 2018.
49. Zhao W, Zhao SP and Zhao YH: MicroRNA-143/-145 in cardiovascular diseases. Biomed Res Int 2015: 531740, 2015.
50. Lovendorf MB, Zibert JR, Gyldenlove M, Ropke MA and Skov L: MicroRNA-223 and miR-143 are important systemic biomarkers for disease activity in psoriasis. J Dermatol Sci 75: 133-139, 2014.
51. Anton L, DeVine A, Sierra LJ, Brown AG and Elovitz MA: miR-143 and miR-145 disrupt the cervical epithelial barrier through dysregulation of cell adhesion, apoptosis and proliferation. Sci Rep 7: 3020, 2017.
52. Liu G, Sun Y, Ji P, Li X, Cogdell D, Yang D, Parker Kerrigan BC, Shmulevich I, Chen K, Sood AK, *et al*: MiR-506 suppresses proliferation and induces senescence by directly targeting the CDK4/6-FOXM1 axis in ovarian cancer. J Pathol 233: 308-318, 2014.
53. Yin M, Ren X, Zhang X, Luo Y, Wang G, Huang K, Feng S, Bao X, Huang K, He X, *et al*: Selective killing of lung cancer cells by miRNA-506 molecule through inhibiting NF-κB p65 to evoke reactive oxygen species generation and p53 activation. Oncogene 34: 691-703, 2015.
54. Li J, Wu H, Li W, Yin L, Guo S, Xu X, Ouyang Y, Zhao Z, Liu S, Tian Y, *et al*: Downregulated miR-506 expression facilitates pancreatic cancer progression and chemoresistance via SPHK1/Akt/NF-κB signaling. Oncogene 35: 5501-5514, 2016.
55. Senderowicz AM: Flavopiridol: The first cyclin-dependent kinase inhibitor in human clinical trials. Invest New Drugs 17: 313-320, 1999.
56. Deep A, Marwaha RK, Marwaha MG, Jyoti, Nandal R and Sharma AK: Flavopiridol as cyclin dependent kinase (CDK) inhibitor: A review. New J Chem 42: 18500-18507, 2018.
57. Sunaga N, Shames DS, Girard L, Peyton M, Larsen JE, Imai H, Soh J, Sato M, Yanagitani N, Kaira K, *et al*: Knockdown of oncogenic KRAS in non-small cell lung cancers suppresses tumor growth and sensitizes tumor cells to targeted therapy. Mol Cancer Ther 10: 336-346, 2011.
58. Berger AH, Brooks AN, Wu X, Shrestha Y, Chouinard C, Piccioni F, Bagul M, Kamburov A, Imielinski M, Hogstrom L, *et al*: High-throughput phenotyping of lung cancer somatic mutations. Cancer Cell 30: 214-228, 2016.
59. Hung MS, Chen IC, Lin PY, Lung JH, Li YC, Lin YC, Yang CT and Tsai YH: Epidermal growth factor receptor mutation enhances expression of vascular endothelial growth factor in lung cancer. Oncol Lett 12: 4598-4604, 2016.
60. Korc M: Driver mutations: A roadmap for getting close and personal in pancreatic cancer. Cancer Biol Ther 10: 588-591, 2010.
61. Timar J and Kashofer K: Molecular epidemiology and diagnostics of KRAS mutations in human cancer. Cancer Metastasis Rev 39: 1029-1038, 2020.
62. Gradiz R, Silva HC, Carvalho L, Botelho MF and Mota-Pinto A: MIA PaCa-2 and PANC-1-pancreas ductal adenocarcinoma cell lines with neuroendocrine differentiation and somatostatin receptors. Sci Rep 6: 21648, 2016.

This work is licensed under a Creative Commons Attribution-NonCommercial-NoDerivatives 4.0 International (CC BY-NC-ND 4.0) License.